Journal of Sound and Vibration (2000) **231**(5), 1321–1338
doi:10.1006/jsvi.1999.2734, available online at http://www.idealibrary.com on IDEAL®

CONTROL OF ADAPTIVE SHELLS WITH THERMAL AND MECHANICAL EXCITATIONS

R. YE

Federal-Mogul Corporation, MI 48034, U.S.A.

AND

H. S. TZOU

Department of Mechanical Engineering, Center for Manufacturing Systems, University of Kentucky, Lexington, KY 40506-0108, *U.S.A.*

(*Received* 4 *March* 1998, *and in final form* 15 *October* 1999)

Shell-type components and structures are very common in many mechanical and structural systems. Modelling and analysis of adaptive piezothermoelastic shell laminates represent high level of sophistication and complexity. Accordingly, a numerical method is developed to investigate the complicated temperature, mechanical, and control interactions of piezothermoelastic shell composites in this study. Constitutive equations and governing equations of a generic piezothermoelastic continuum are defined first. Strain–displacement relations, electric field–potential relations, thermal gradient–temperature relations of laminated shell composites are then defined. A new piezothermoelastic composite triangular shell finite element is formulated and developed. Matrix equations of the piezothermoelastic shell laminate are derived, in which mechanical, temperature, and electric force vectors are also defined. The electric force vector is used to active control of the shell laminates. Finite element solutions of a piezoelectric laminated composite plate are compared with experimental data and numerical solutions first. Distributed control of a piezoelectric laminated semicircular shell subjected to mechanical and temperature (thermal shock) excitations is investigated and control effectiveness evaluated.

1. INTRODUCTION

Recent research and development of smart structures and structronic systems has promised new design opportunities for the next-generation high-performance mechanical and structural systems, ranging from micro-electromechanical systems to aircrafts and aerospace systems. There are a number of active electromechanical materials, such as piezoelectrics, shape-memory alloys, electrostrictive materials, electromagnetostrictive materials, electro- and magneto-rheological materials, etc., investigated today [1]. Piezoelectric materials are probably the most popular active material used in both sensor and actuator applications. Classical distributed sensing and control characteristics have been investigated in recent years [2].

0022-460X/00/151321 + 18 $35.00/0

Distributed control effects of one-dimensional and two-dimensional planar structures, e.g., beams and plates, are studied and compared [3–8], and also rings and shells [9–12]. Temperature influences on piezoelectric sensors and actuators of beam-type precision devices have been studied based on a thin piezothermoelastic solid finite element [13]. Shell-type components and structures are very common in many mechanical and structural systems, e.g., nozzles, pressure vessels, storage tanks, rockets, antenna dishes, etc. Modelling and analysing of adaptive piezothermoelastic shell laminates represents a high level of sophistication and complexity [2, 11]. In general, theoretical solutions of shell composites are scarce and experiments are also difficult to conduct. This paper is to investigate the modelling and active vibration control of piezoelectric laminated shells subjected to mechanical and temperature (thermal shock) excitations using a numerical technique. Fundamental piezothermoelasticity is reviewed first and followed by the development of a new piezothermoelastic triangle composite shell finite element including the temperature effect, extended from the piezoelastic shell element [14]. Distributed vibration controls of mechanical and/or thermal shock-induced vibrations of plate and shells are investigated and compared.

2. LINEAR PIEZOTHERMOELASTICITY

For a piezothermoelastic medium, with a volume V and a limited surface area S, subjected to combined thermal, electric, and mechanical excitations, the linear governing equations, including the coupling among deformation, electric potential, and temperature fields, can be grouped as follows [13, 15].

Governing equations

$$T_{ij,j} + f_{bi} = \rho \ddot{U}_i, \qquad D_{i,i} = 0, \qquad \kappa_{ij}\theta_{ij} - \theta_0 \dot{\xi} = 0, \tag{1–3}$$

where T_{ij}, D_i, θ, $\ddot{U}_i$, ξ, ρ, f_{bi}, κ_{ij}, and θ_0 denote the stress, electric displacement, temperature, acceleration, entropy density, mass density, body force, heat conductivity coefficient, and reference temperature respectively. Note that Einstein's summation convention is used in the expressions. The system will be highly non-linear only at the most initial time of thermal shock. Because the controlled responses at a certain period of time are of interest in this study, the system is still considered to be linear.

Constitutive equations

$$T_{ij} = c_{ijkl}^{E,\theta}(S_{kl} - S_{kl}^0) - e_{mij}^{\theta} E_m - \lambda_{ij}^{E}\theta, \tag{4}$$

$$D_n = e_{nkl}^{\theta}(S_{kl} - S_{kl}^0) + \varepsilon_{nm}^{S,\theta} E_m + p_n^S \theta, \tag{5}$$

$$\xi = \lambda_{kl}^{E}(S_{kl} - S_{kl}^0) + p_m^S E_m + \alpha_v \theta, \tag{6}$$

where $c_{ijkl}^{E,\theta}$, e_{mij}^{θ}, λ_{ij}^{E}, $\varepsilon_{nm}^{S,\theta}$, p_n^s, S_{ki} and S_{kl}^0 denote the elastic moduli, piezoelectric coefficient, temperature stress coefficient, dielectric constant, pyroelectric constant,

strain, and initial strain respectively; α_v is a material constant ($\alpha_v = \rho c_v \theta_0^{-1}$) where c_v is the specific heat at constant volume. In addition, the superscripts E, θ and S denote the coefficients defined at a constant electric field, temperature and strain respectively.

Boundary conditions on boundary surfaces

$$U_i = \bar{U}_i, \qquad T_{ij} l_j = f_i, \tag{7, 8}$$

$$\phi = \bar{\phi}, \qquad D_i l_i = -Q, \tag{9, 10}$$

$$\theta = \bar{\theta}, \qquad \kappa_{ij} \theta_{,j} l_i = q_s, \tag{11, 12}$$

$$-\kappa_{ij} \theta_{,j} l_i = q_h = h_v(\theta + \theta_0 - \theta_\infty), \tag{13}$$

where U_i is the displacement, ϕ is the electric potential, f_i is the surface force, Q is the charge, q_s and q_h are the surface heat flux, h_v is the thermal convection coefficient, l_i is the direction cosine components, $(\bar{\cdot})$ denotes a known boundary value, and θ_∞ is the environment temperature.

Using the weighted residual method and introducing arbitrary weighting quantities δU_i, $\delta\phi$, and $\delta\theta$ [16], one can rewrite the weak form of the equilibrium equations (1) to (3) as

$$\int_V \delta U_i (T_{ij,j} + f_{bi} - \rho \ddot{U}_i)\, \mathrm{d}V = 0, \quad \int_V \delta\phi D_{i,i}\, \mathrm{d}V = 0, \quad \int_V \delta\theta (\kappa_{ij}\theta_{,ij} - \theta_0 \dot{\xi})\, \mathrm{d}V = 0, \tag{14–16}$$

where the quantities δU_i, $\delta\phi$ and $\delta\theta$ can be defined as the virtual displacement, electric potential and temperature, respectively. Integrating each term by parts, taking into account of boundary conditions in equations (7)–(13), and noting that $\delta U_i = 0$ on S_u, $\delta\phi = 0$ on S_ϕ, and $\delta\theta = 0$ on S_θ, one can simplify equations (14)–(16) to

$$\int_V T_{ij} \delta S_{ij}\, \mathrm{d}V - \int_{S_T} f_i \delta U_i\, \mathrm{d}S - \int_V (f_{bi} - \rho \ddot{U}_i) \delta U_i\, \mathrm{d}V = 0. \tag{17}$$

$$\int_V D_i \delta E_i\, \mathrm{d}V - \int_{S_D} Q \delta\phi\, \mathrm{d}S = 0, \tag{18}$$

$$\int_V \kappa_{ij} \theta_{,j} \delta\theta_{,j}\, \mathrm{d}V + \int_V \theta_0 \dot{\xi} \delta\theta\, \mathrm{d}V - \int_{S_{q_k}} q_s \delta\theta\, \mathrm{d}S$$

$$+ \int_{S_{qh}} h_v(\theta + \theta_0 - \theta_\infty) \delta\theta\, \mathrm{d}S = 0. \tag{19}$$

Note that equations (17)–(19) are the virtual work expressions of the piezothermoelastic continuum.

3. LAMINATED PIEZOELASTIC SHELLS

A laminated piezoelastic shell is composed of N laminate, and each of the lamina can be either elastic material or piezoelastic material. It is assumed that the piezoelastic shell is exposed to coupled mechanical, electrical, and thermal excitations. All relations of displacement, strain, electric, and temperature fields are established in an orthogonal curvilinear co-ordinate system $(\alpha_1, \alpha_2, \alpha_3)$. Considering small deformation of the laminated piezoelastic shell, one can derive the strain S_{ij}, electric field E_i, and temperature gradient g_i equations. The strain–displacement relations, electric field–electric potential relations, and temperature gradient–temperature relations in a tri-orthogonal shell co-ordinate system are defined as follows:

$$S_{11} = \frac{1}{(1 + \alpha_3/R_1)A_1}\left[\frac{\partial U_1}{\partial \alpha_1} + \frac{1}{A_2}\frac{\partial A_1}{\partial \alpha_2}U_2 + \frac{A_1}{R_1}U_3\right], \tag{20}$$

$$S_{22} = \frac{1}{(1 + \alpha_3/R_2)A_2}\left[\frac{\partial U_2}{\partial \alpha_2} + \frac{1}{A_1}\frac{\partial A_2}{\partial \alpha_1}U_1 + \frac{A_2}{R_2}U_3\right], \tag{21}$$

$$S_{33} = \frac{\partial U_3}{\partial \alpha_3}, \tag{22}$$

$$S_{12} = \frac{1}{2(1 + \alpha_3/R_1)A_1}\left[\frac{\partial U_2}{\partial \alpha_1} - \frac{1}{A_2}\frac{\partial A_1}{\partial \alpha_2}U_1\right] + \frac{1}{2(1 + \alpha_3/R_2)A_2}\left[\frac{\partial U_1}{\partial \alpha_2} - \frac{1}{A_1}\frac{\partial A_2}{\partial \alpha_1}U_2\right], \tag{23}$$

$$S_{13} = \frac{1}{2(1 + \alpha_3/R_1)A_1}\left[\frac{\partial U_3}{\partial \alpha_1} - \frac{A_1}{R_1}U_1\right] + \frac{1}{2}\frac{\partial U_1}{\partial \alpha_3}, \tag{24}$$

$$S_{23} = \frac{1}{2(1 + \alpha_3/R_2)A_2}\left[\frac{\partial U_3}{\partial \alpha_2} - \frac{A_2}{R_2}U_2\right] + \frac{1}{2}\frac{\partial U_2}{\partial \alpha_3}, \tag{25}$$

$$E_1 = -\frac{1}{(1 + \alpha_3/R_1)A_1}\frac{\partial \phi}{\partial \alpha_1}, \quad E_2 = -\frac{1}{(1 + \alpha_3/R_2)A_2}\frac{\partial \phi}{\partial \alpha_2},$$

$$E_3 = -\frac{\partial \phi}{\partial \alpha_3}, \tag{26–28}$$

$$g_1 = -\frac{1}{(1+\alpha_3/R_1)A_1}\frac{\partial\theta}{\partial\alpha_1}, \quad g_2 = -\frac{1}{(1+\alpha_3/R_2)A_2}\frac{\partial\theta}{\partial\alpha_2},$$

$$g_3 = -\frac{\partial\theta}{\partial\alpha_3}, \tag{29–31}$$

where S_{ij}, E_i, and g_i denote the strains, electric fields and temperature gradients respectively. R_1 and R_2 are the radii of principal curvature: A_1 and A_2 are the Lamé parameters.

4. PIEZOTHERMOELASTIC FINITE ELEMENT FORMULATION

A new 12-node, 60 degree-of-freedom curved triangular laminated piezothermoelastic shell element is developed. The assumptions of layerwise constant shear angle and linear variation along thickness of each layer are used in the finite element derivations [14]. Figure 1 illustrates the triangular shell element.

Thus, for an arbitrary layer i, the displacements $U_1^{(i)}(\gamma)$, $U_2^{(i)}(\gamma)$, and $U_3^{(i)}(\gamma)$, electric potential $\phi^{(i)}(\gamma)$, and temperature $\theta^{(i)}(\gamma)$ fields can be expressed as

$$U_1^{(i)}(\gamma), = \bar{U}_1^{(i)}\left(1-\frac{\gamma}{h_i}\right) + \bar{U}_1^{(i+1)}\frac{\gamma}{h_i}, \tag{32}$$

$$U_2^{(i)}(\gamma), = \bar{U}_2^{(i)}\left(1-\frac{\gamma}{h_i}\right) + \bar{U}_2^{(i+1)}\frac{\gamma}{h_i}, \tag{33}$$

$$U_3^{(i)}(\gamma), = \bar{U}_3^{(i)}\left(1-\frac{\gamma}{h_i}\right) + \bar{U}_3^{(i+1)}\frac{\gamma}{h_i}, \tag{34}$$

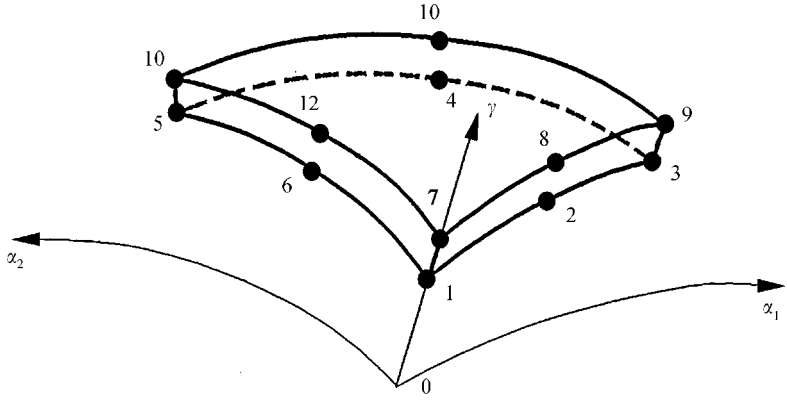

Figure 1. Triangular piezothermoelastic shell composite element.

$$\phi^{(i)}(\gamma), = \bar{\phi}^{(i)}\left(1 - \frac{\gamma}{h_i}\right) + \bar{\phi}^{(i+1)}\frac{\gamma}{h_i}, \tag{35}$$

$$\theta^{(i)}(\gamma), = \bar{\theta}^{(i)}\left(1 - \frac{\gamma}{h_i}\right) + \bar{\theta}^{(i+1)}\frac{\gamma}{h_i}. \tag{36}$$

where γ is a transverse co-ordinate defined for the ith layer. Equations (32)–(36) can be simply written as

$$\{U^{(i)}(\gamma)\} = [N_u^{(i)}(\gamma)]\{\bar{U}^{(i)}\}, \quad \phi^{(i)}(\gamma) = [N_\phi^{(i)}(\gamma)]\{\bar{\phi}^{(i)}\}, \quad \theta^{(i)}(\gamma) = [N_\theta^{(i)}(\gamma)]\{\bar{\theta}^{(i)}\}, \tag{37–39}$$

where $\{U^{(i)}(\gamma)\} = \{U_1^{(i)}(\gamma), U_2^{(i)}(\gamma), U_3^{(i)}(\gamma)\}^t$ is a displacement vector of any point in the ith layer. $\{\bar{U}^{(i)}\} = \{\bar{U}_1^{(i)}, \bar{U}_2^{(i)}, \bar{U}_3^{(i)}, \bar{U}_1^{(i+1)}, \bar{U}_2^{(i+1)}, \bar{U}_3^{(i+1)}\}^t$, $\{\bar{\phi}^{(i)}\} = \{\bar{\phi}^{(i)}, \bar{\phi}^{(i+1)}\}^t$, and $\{\bar{\theta}^{(i)}\} = \{\bar{\theta}^{(i)}, \bar{\theta}^{(i+1)}\}^t$, are the displacements, electric potential, and temperature vectors of the ith and $(i+1)$th interfaces along the curvilinear co-ordinate axes. $[N_u^{(i)}(\gamma)]$, $[N_\phi^{(i)}(\gamma)]$, and $[N_\theta^{(i)}(\gamma)]$ are the shape functions in terms of the co-ordinate γ. h_i is the thickness of the ith layer. The interpolation functions of the surface-parallel displacements, electric potential and temperature in each triangular region at the ith or $(i+1)$th interface are chosen to be continuous piecewise quadratic in the form

$$\begin{Bmatrix} \{\bar{U}^{(i)}\} \\ \{\bar{\phi}^{(i)}\} \\ \{\bar{\theta}^{(i)}\} \end{Bmatrix} = a_1\alpha_1^2 + a_2\alpha_2^2 + a_3\alpha_1\alpha_2 + a_4\alpha_1 + a_5\alpha_2 + a_6, \tag{40}$$

where $a_i (i = 1, \ldots, 6)$ are constants, and $\alpha_i (i = 1, 2, 3)$ are the global co-ordinates. Due to the continuity across the edge between two adjacent triangles, equation (40) becomes

$$\bar{U}_1^{(i)} = \{N\}^t\{U_1^{(i)}\}, \qquad \bar{U}_2^{(i)} = \{N\}^t\{U_2^{(i)}\}, \qquad \bar{U}_3^{(i)} = \{N\}^t\{U_3^{(i)}\}, \tag{41–43}$$

$$\bar{\phi}^{(i)} = \{N\}^t\{\phi^{(i)}\}, \qquad \bar{\theta}^{(i)} = \{N\}^t\{\theta^{(i)}\}, \tag{44, 45}$$

where $\{U_1^{(i)}\} = \{U_{11}^i, \ldots, U_{16}^i\}^t$, $\{U_2^{(i)}\} = \{U_{21}^i, \ldots, U_{26}^i\}^t$, $\{U_3^{(i)}\} = \{U_{31}^i, \ldots, U_{36}^i\}^t$, $\{\phi^{(i)}\} = \{\phi_1^i, \ldots, \phi_6^i\}^t$, and $\{\theta^{(i)}\} = \{\theta_1^i, \ldots, \theta_6^i\}^t$ are the nodal displacement, electric potential, and temperature vectors of the element. $\{N\}$ is the quadratic shape function. Substituting equations (41)–(45) into equations (37)–(39) leads to the following expressions of $\{\bar{U}^{(i)}\}$, $\{\bar{\phi}^{(i)}\}$, and $\{\bar{\theta}^{(i)}\}$:

$$\{\bar{U}^{(i)}\} = [N_{u_i}(\alpha_1, \alpha_2)]\{U_j^{(i)})\}, \quad \{\bar{\phi}^{(i)}\} = [N_{\phi_j}(\alpha_1, \alpha_2)]\{\phi_j^{(i)}\},$$

$$\{\bar{\theta}^{(i)}\} = [N_{\theta_j}(\alpha_1, \alpha_2)]\{\theta_j^{(i)}\}, \tag{46–48}$$

where $\{U_j^{(i)}\} = \{U_{11}^i, U_{21}^i, U_{31}^i, \ldots, U_{16}^i, U_{26}^i, U_{36}^i, U_{11}^{i+1}, U_{21}^{i+1}, U_{31}^{i+1}, \ldots, U_{16}^{i+1}, U_{26}^{i+1}, U_{36}^{i+1}\}^t$, $\{\phi_j^{(i)}\} = \{\phi_1^i, \ldots, \phi_6^i, \phi_1^{i+1}, \ldots, \phi_6^{i+1}\}^t$, and $\{\theta_j^{(i)}\} = \{\theta_1^i, \ldots, \theta_6^i, \theta_1^{i+1}, \ldots, \theta_6^{i+1}\}^t$, are the nodal displacements, nodal electric potential, and nodal temperature of the jth planar layer element located on the jth layer respectively. $[N_{u_j}(\alpha_1, \alpha_2)]$, $[N_{\phi_j}(\alpha_1, \alpha_2)]$, and $[N_{\theta_j}(\alpha_1, \alpha_2)]$, are the shape functions of co-ordinates α_1 and α_2. Writing equations (20)–(31) in terms of nodal variables of the element gives

$$\{S^{(i)}(\gamma)\} = [L_u^{(i)}][N_u^{(i)}(\gamma)][N_{u_j}(\alpha_1, \alpha_2)]\{U_j^{(i)}\}$$

$$= [B_u^{(i)}(\gamma)][B_{u_j}(\alpha_1, \alpha_2)]\{U_j^{(i)}\}, \tag{49}$$

$$\{E^{(i)}(\gamma)\} = -[L_\phi^{(i)}][N_\phi^{(i)}(\gamma)][N_{\phi_j}(\alpha_1, \alpha_2)]\{\phi_j^{(i)}\}$$

$$= -[B_\phi^{(i)}(\gamma)][B_{\phi_j}(\alpha_1, \alpha_2)]\{\phi_j^{(i)}\}, \tag{50}$$

$$\{g^{(i)}(\gamma)\} = -[L_\theta^{(i)}][N_\theta^{(i)}(\gamma)][N_{\theta_j}(\alpha_1, \alpha_2)]\{\theta_j^{(i)}\}$$

$$= -[B_\theta^{(i)}(\gamma)][B_{\theta_j}(\alpha_1, \alpha_2)]\{\theta_j^{(i)}\}. \tag{51}$$

Substituting equations (4)–(6), (37)–(39), and (46)–(51) into equations (17)–(19), one can derive the nodal governing equations of the jth (planar) element located on the ith (thickness) layer in a matrix form:

$$\begin{bmatrix} [M_{uu_j}^{(i)}] & 0 & 0 \\ 0 & 0 & 0 \\ 0 & 0 & 0 \end{bmatrix} \begin{Bmatrix} \{\ddot{U}_j^{(i)}\} \\ \{\ddot{\phi}_j^{(i)}\} \\ \{\ddot{\theta}_j^{(i)}\} \end{Bmatrix} + \begin{bmatrix} [C_{uu_j}^{(i)}] & 0 & 0 \\ 0 & 0 & 0 \\ \theta_0[K_{\theta u_j}^{(i)}] & -\theta_0[K_{\theta\phi_j}^{(i)}] & [H_{\theta\theta_j}^{(i)}] \end{bmatrix} \begin{Bmatrix} \{\dot{U}_j^{(i)}\} \\ \{\dot{\phi}_j^{(i)}\} \\ \{\dot{\theta}_j^{(i)}\} \end{Bmatrix}$$

$$+ \begin{bmatrix} [K_{uu_j}^{(i)}] & [K_{u\phi_j}^{(i)}] & -[K_{u\theta_j}^{(i)}] \\ [K_{\phi u_j}^{(i)}] & [K_{\phi\phi_j}^{(i)}] & [K_{\phi\theta_j}^{(i)}] \\ 0 & 0 & [K_{\theta\theta_j}^{(i)}] \end{bmatrix} \begin{Bmatrix} \{U_j^{(i)}\} \\ \{\phi_j^{(i)}\} \\ \{\theta_j^{(i)}\} \end{Bmatrix} = \begin{Bmatrix} \{F_{u_j}^{(i)}\} \\ \{F_{\phi_j}^{(i)}\} \\ \{F_{\theta_j}^{(i)}\} \end{Bmatrix}, \tag{52}$$

where $[M_{uu_j}^{(i)}]$ is the mass matrix: $[C_{uu_j}^{(i)}]$ and $[H_{\theta\theta_j}^{(i)}]$ are the damping matrices: $[K_{xy_j}^{(i)}]$ (where x & $y = u$, ϕ, and θ) are the stiffness matrices defined for the displacement, electric potential, and temperature fields: $\{F_{u_j}^{(i)}\}$, $\{F_{\phi_j}^{(i)}\}$, and $\{F_{\theta_j}^{(i)}\}$ are the mechanical, electric, and thermal excitation. Detailed element matrices of a laminated piezothermoelastic shell element are presented as follows:

$$[M_{uu_j}^{(i)}] = \int_{S_j} [N_{u_j}(\alpha_1, \alpha_2)]^t \left(\int_{\gamma=0}^{h_i} [N_u^{(i)}(\gamma)]^t \rho^{(i)} [N_u^{(i)}(\gamma)] B_1^i B_2^i \, d\gamma \right)$$

$$\times [N_{u_j}(\alpha_1, \alpha_2)] A_1 A_2 \, d\alpha_1 \, d\alpha_2, \tag{53}$$

$$[K_{uu_j}^{(i)}] = \int_{S_j} [B_{u_j}(\alpha_1, \alpha_2)]^t \left(\int_{\gamma=0}^{h_i} [B_u^{(i)}(\gamma)]^t [\bar{c}^{(i)}] [B_u^{(i)}(\gamma)] B_1^i B_2^i \, \mathrm{d}\gamma \right)$$

$$\times [B_{u_j}(\alpha_1, \alpha_2)] A_1 A_2 \, \mathrm{d}\alpha_1 \, \mathrm{d}\alpha_2, \tag{54}$$

$$[K_{u\phi_j}^{(i)}] = \int_{S_j} [B_{u_j}(\alpha_1, \alpha_2)]^t \left(\int_{\gamma=0}^{h_i} [B_u^{(i)}(\gamma)]^t [\bar{e}^{(i)}] [B_\phi^{(i)}(\gamma)] B_1^i B_2^i \, \mathrm{d}\gamma \right)$$

$$\times [B_{\phi_j}(\alpha_1, \alpha_2)] A_1 A_2 \, \mathrm{d}\alpha_1 \, \mathrm{d}\alpha_2, \tag{55}$$

$$[K_{u\theta_j}^{(i)}] = \int_{S_j} [B_{u_j}(\alpha_1, \alpha_2)]^t \left(\int_{\gamma=0}^{h_i} [B_u^{(i)}(\gamma)]^t [\bar{\lambda}^{(i)}] [N_\theta^{(i)}(\gamma)] B_1^i B_2^i \, \mathrm{d}\gamma \right)$$

$$\times [N_{\theta_j}(\alpha_1, \alpha_2)] A_1 A_2 \, \mathrm{d}\alpha_1 \, \mathrm{d}\alpha_2, \tag{56}$$

$$[K_{\phi\phi_j}^{(i)}] = -\int_{S_j} [B_{\phi_j}(\alpha_1, \alpha_2)]^t \left(\int_{\gamma=0}^{h_i} [B_\phi^{(i)}(\gamma)]^t [\bar{\varepsilon}^{(i)}] [B_\phi^{(i)}(\gamma)] B_1^i B_2^i \, \mathrm{d}\gamma \right)$$

$$\times [B_{\phi_j}(\alpha_1, \alpha_2)] A_1 A_2 \, \mathrm{d}\alpha_1 \, \mathrm{d}\alpha_2, \tag{57}$$

$$[K_{\phi\theta_j}^{(i)}] = \int_{S_j} [B_{\phi_j}(\alpha_1, \alpha_2)]^t \left(\int_{\gamma=0}^{h_i} [B_\phi^{(i)}(\gamma)]^t [\bar{p}^{(i)}] [N_\theta^{(i)}(\gamma)] B_1^i B_2^i \, \mathrm{d}\gamma \right)$$

$$\times [N_{\theta_j}(\alpha_1, \alpha_2)] A_1 A_2 \, \mathrm{d}\alpha_1 \, \mathrm{d}\alpha_2, \tag{58}$$

$$[K_{\theta\theta_j}^{(i)}] = \int_{S_j} [B_{\theta_j}(\alpha_1, \alpha_2)]^t \left(\int_{\gamma=0}^{h_i} [B_\theta^{(i)}(\gamma)]^t [\bar{\kappa}_{ij}^{(i)}] [B_\theta^{(i)}(\gamma)] B_1^i B_2^i \, \mathrm{d}\gamma \right)$$

$$\times [B_{\theta_j}(\alpha_1, \alpha_1)] A_1 A_2 \, \mathrm{d}\alpha_1 \, \mathrm{d}\alpha_2 + \int_{S_{q_{ij}}} h_v [N_{\theta_j}(\alpha_1, \alpha_2)]^t [N_\theta^{(i)}(\gamma = h_x)]^t$$

$$\times [N_\theta^{(i)}(\gamma = h_x)] [N_{\theta_j}(\alpha_1, \alpha_2)] B_1^i(\gamma = h_x) B_2^i(\gamma = h_x) \, \mathrm{d}\gamma) A_1 A_2 \, \mathrm{d}\alpha_1 \, \mathrm{d}\alpha_2, \tag{59}$$

$$[H_{\theta\theta_j}^{(i)}] = \int_{S_j} [N_{\theta_j}(\alpha_1, \alpha_2)]^t \left(\int_{\gamma=0}^{h_i} [N_\theta^{(i)}(\gamma)]^t \theta_0 \alpha_v^{(i)} [N_\theta^{(i)}(\gamma)] B_1^i B_2^i \, \mathrm{d}\gamma \right)$$

$$\times [N_{\theta_j}(\alpha_1, \alpha_2)] A_1 A_2 \, \mathrm{d}\alpha_1 \, \mathrm{d}\alpha_2, \tag{60}$$

$$[K_{\theta u_j}^{(i)}] = [K_{u\theta_j}^{(i)}]^t, \qquad [K_{\phi u_j}^{(i)}] = [K_{u\phi_j}^{(i)}]^t, \qquad [K_{\theta\phi_j}^{(i)}] = [K_{\phi\theta_j}^{(i)}]^t, \tag{61}$$

$$[F_{u_j}^{(i)}] = \int_{S_j} [N_{u_j}(\alpha_1, \alpha_2)]^t [N_u^{(i)}(\gamma = h_x)]^t \{ f^{(i)} \} B_1^i(\gamma = h_x) B_2^i(\gamma = h_x) A_1 A_2 \, d\alpha_1 \, d\alpha_2$$

$$+ \int_{S_j} [N_{u_j}(\alpha_1, \alpha_2)]^t \left(\int_{\gamma=0}^{h_i} [N_u^{(i)}(\gamma)]^t \{ f_b^{(i)} \} B_1^i B_2^i \, d\gamma \right) A_1 A_2 \, d\alpha_1 \, d\alpha_2, \quad (62)$$

$$[F_{\phi_j}^{(i)}] = - \int_{S_j} [N_{\phi_j}(\alpha_1, \alpha_2)]^t [N_\phi^{(i)}(\gamma = h_x)]^t Q^i B_1^i(\gamma = h_x) B_2^i(\gamma = h_x) A_1 A_2 \, d\alpha_1 \, d\alpha_2, \quad (63)$$

$$[F_{\theta_j}^{(i)}] = \int_{S_{qS_j}} [N_{\theta_j}(\alpha_1, \alpha_2)]^t [N_\theta^{(i)}(\gamma = h_x)]^t q_s B_1^i(\gamma = h_x) B_2^i(\gamma = h_x) A_1 A_2 \, d\alpha_1 \, d\alpha_2$$

$$- \int_{S_{qh_j}} [N_{\theta_j}(\alpha_1, \alpha_2)]^t [N_\theta^{(i)}(\gamma = h_x)]^t h_v \theta_\infty B_1^i(\gamma = h_x) B_2^i(\gamma = h_x) A_1 A_2 \, d\alpha_1 \, d\alpha_2, \quad (64)$$

where $\{ f^{(i)} \} = \{ f_1^{(i)}, f_2^{(i)}, f_3^{(i)} \}^t$ and $\{ f_b^{(i)} \} = \{ f_{b1}^{(i)}, f_{b2}^{(i)}, f_{b3}^{(i)} \}^t$ are the surface force and body force along the curvilinear co-ordinate axes respectively, Q^t is the electric charge applied on the surfaces of piezoelectric layers, q_s is the heat flux on the top and bottom surfaces of shell structures, h_v is the thermal convection coefficient: and the thickness $0{\cdot}0 \leqslant h_x \leqslant h_i$. The element damping matrix $[C_{uu_j}^{(i)}]$ is assumed to be proportional to the stiffness and mass matrices:

$$[C_{uu_j}^{(i)}] = \alpha [M_{uu_j}^{(i)}] + \beta [K_{uu_j}^{(i)}]. \quad (65)$$

where α and β are Rayleigh's coefficients and are related by [17]

$$\alpha + \beta \omega_i^2 = 2 \xi_i \omega_i. \quad (66)$$

where ξ_i and ω_i are the initial damping ratio and natural frequencies. If two damping ratios and two natural frequencies are specified, equation (66) results in an exact solution for α and β. If more than two damping ratios and frequencies are specified, a least-squares solution procedure can be used to determine α and β. The developed new piezothermoelastic shell element and associated finite element code are used in active control of plates and shells presented next.

5. NUMERICAL EXAMPLES

Two examples are presented in this section. One is the static deflection analysis of a piezoelectric laminated composite plate in which the finite element solutions are compared with published finite element and experimental results. The other is the distributed vibration control of a semicircular shell subjected to mechanical and temperature (thermal shock) excitations. The control part has been well established and detailed discussion about control can be found in papers [2, 3, 14]. In this study, the negative velocity feedback is used in all examples.

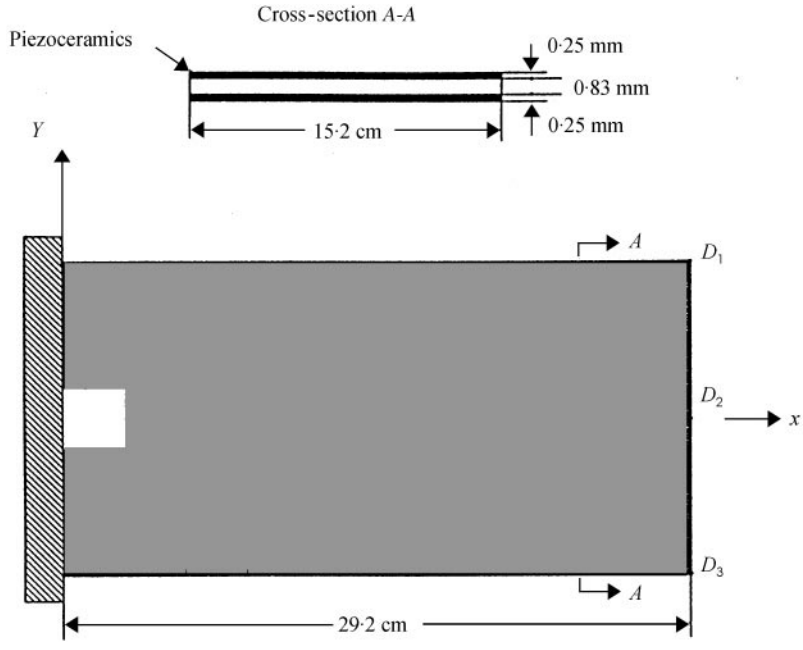

Figure 2. Piezoelectric laminated plate composite.

5.1. CANTILEVER PLATE WITH PIEZOELECTRIC ACTUATOR

Application of piezoelectric film as distributed actuators to piezoelectric laminated composite plates are evaluated. In this case, a cantilevered laminated $[0/\pm 45]_S$ composite plate with distributed G-1195 piezoelectric ceramics bonded on the surfaces of the composite plate is studied. Dimensions of the laminated plate are shown in Figure 2.

A constant field (394 V/mm) is applied to the piezoelectric film laminated on each side of the plate. Displacement of the plate along the two parallel edges and the centerline are calculated and resolved into three non-dimensional displacements: $W_1 = D_2/B$, $W_2 = (D_3 - D_1)/B$, $W_3 = [D_2 - (D_3 + D_1)/2]/B$, where $B = 15{\cdot}2$ cm is the width of the plate, D_1, D_2 and D_3 are the lateral deflections of three points in the free edge shown in Figure 2, and W_1, W_2, and W_3 are the longitudinal bending, lateral twisting, and transverse bending deflections respectively. Finite element solutions are compared with the experimental results [4] and other finite element results [6] in Figure 3. Figure 3(a) indicates the out-of-plane longitudinal bending W_1 as a function of the position. The solid line is the solution based on the finite element model, which agrees with the experiment result very well. Figures 3(b) and 3(c) show the lateral twisting W_2 and transverse bending W_3 as a function of the position. In spite of the scattering of the experiment data, the solutions still compare reasonably with the experiments and other numerical solutions. Note that the order of magnitudes in Figures 3(b) and (c) is different from that in Figure 3(a). Thus, it is reasonable to state that the newly developed finite element code can be confidently used to analyze piezoelectrical-laminated composite structures.

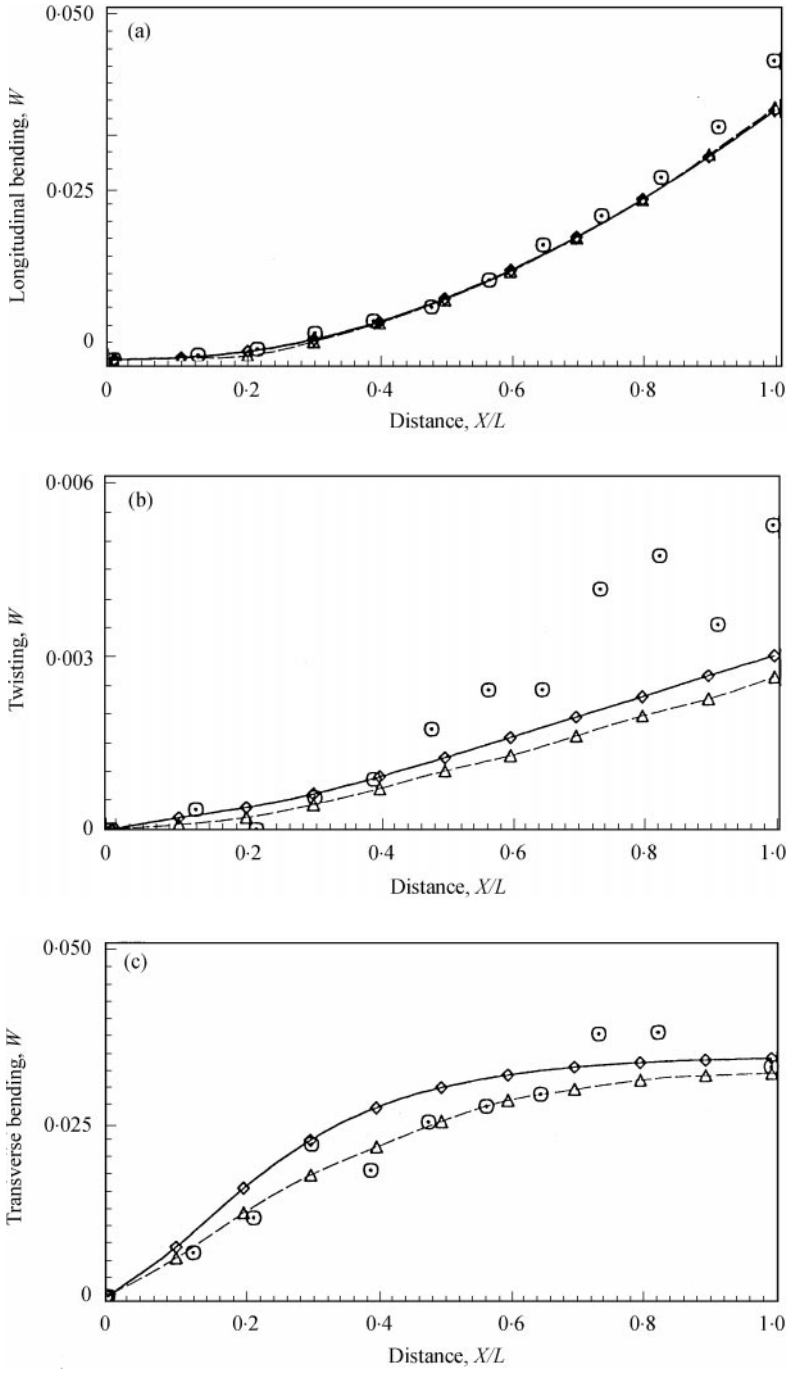

Figure 3. Static deflections of the composite plate: (a) longitudinal bending: (b) lateral twisting, and (c) transverse bending; ⇨, experiment [4]; △, FEM [6]; and ◇, present.

5.2. DISTRIBUTED CONTROL OF A CANTILEVER SEMICIRCULAR SHELL

Vibration control of shells differs from that of plates because of the coupling of bending and membrane oscillations. In this case, multiple pairs of sensors and actuators are used to sense and control the shell vibration. Four strip sensor/actuator pairs are laminated on a semicircular shell, in which the bottom strips serve as sensors and top strips serve as actuators. Figure 4(a). For each pair of sensor/actuator, an output signal is provided by the bottom sensor, amplified, and then fed back to the top actuator resulting in control forces/moments for vibration control of the semicircular shell. The piezoelectric material is the polymeric polyvinylidene fluoride (PVDF) and the elastic shell is made of steel. The elastic shell is 200 mm long, 150 mm wide, and 0·8 mm thick, and its inner radius is 63·662 mm. Each top PVDF actuator on the outer shell surface is 202·5 mm long, 15 mm wide, and 28 μm thick. Each bottom PVDF sensor on the inner surface is 200 mm long, 15 mm wide, and 28 μm thick. All materil properties are given in Table 1. Because of the difficulty to obtain the properties varied with temperature, all material properties in the table assumed constants.

For finite element analysis, the elastic shell is divided into a 10×10 mesh, and each sensor/actuator strip is 1×10, Figure 4(b). Thus, there are 200 triangular elastic elements for the elastic shell and 80 triangular piezothermoelastic elements for four PVDF sensor/actuator strips. Free-vibration eigenvalue analysis suggests that the first five natural frequencies are $f_1 = 37{\cdot}87$ Hz (bending mode), $f_2 = 138{\cdot}55$ Hz (2nd bending mode), $f_3 = 471{\cdot}27$ Hz (3rd bending mode), $f_4 = 894{\cdot}91$ Hz (4th bending mode), and $f_5 = 1054{\cdot}25$ Hz (coupled bending/torsion mode). The initial damping of the shell is assumed to be 0·2%. Active vibration control of the shell with mechanical and temperature (thermal shock) excitations are investigated next.

5.2.1. *Control of snap-back responses*

Free and controlled snap-back responses of the shell with an initial displacement of 1 cm at the free and are studied. A set of feedback gains ω_1, $2{\cdot}0\omega_1$, and $5{\cdot}5\omega_1$ are used, respectively, for the negative velocity feedback control. Free response and a controlled response (gain $= 2{\cdot}0\omega_1$) of node-1 (see Figure 4) are shown in Figures 5(a) and 5(b) respectively. The 2-D controlled end response at gain $= 2{\cdot}0\omega_1$ is also presented in Figure 5(c) where TIME is time (s), Y is the free end width (m), and DISP is the displacement response (cm). It is observed that the higher modes are also coupled with the fundamental mode (the bending mode) at the time between 0·0 and 0·2 s, and they quickly vanish because of the combined effect of damping and frequency.

The decay envelopes of node 1 for different control gains are plotted and compared in Figure 6. Note that the shell response is better controlled with the increased control gain.

5.2.2. *Control of thermal excitation*

Controlled responses of the shell with thermal shock excitations are also studied. The shell is instantly exposed to a thermal shock temperature difference between the bottom and the top surfaces. It is assumed that the temperature of the top

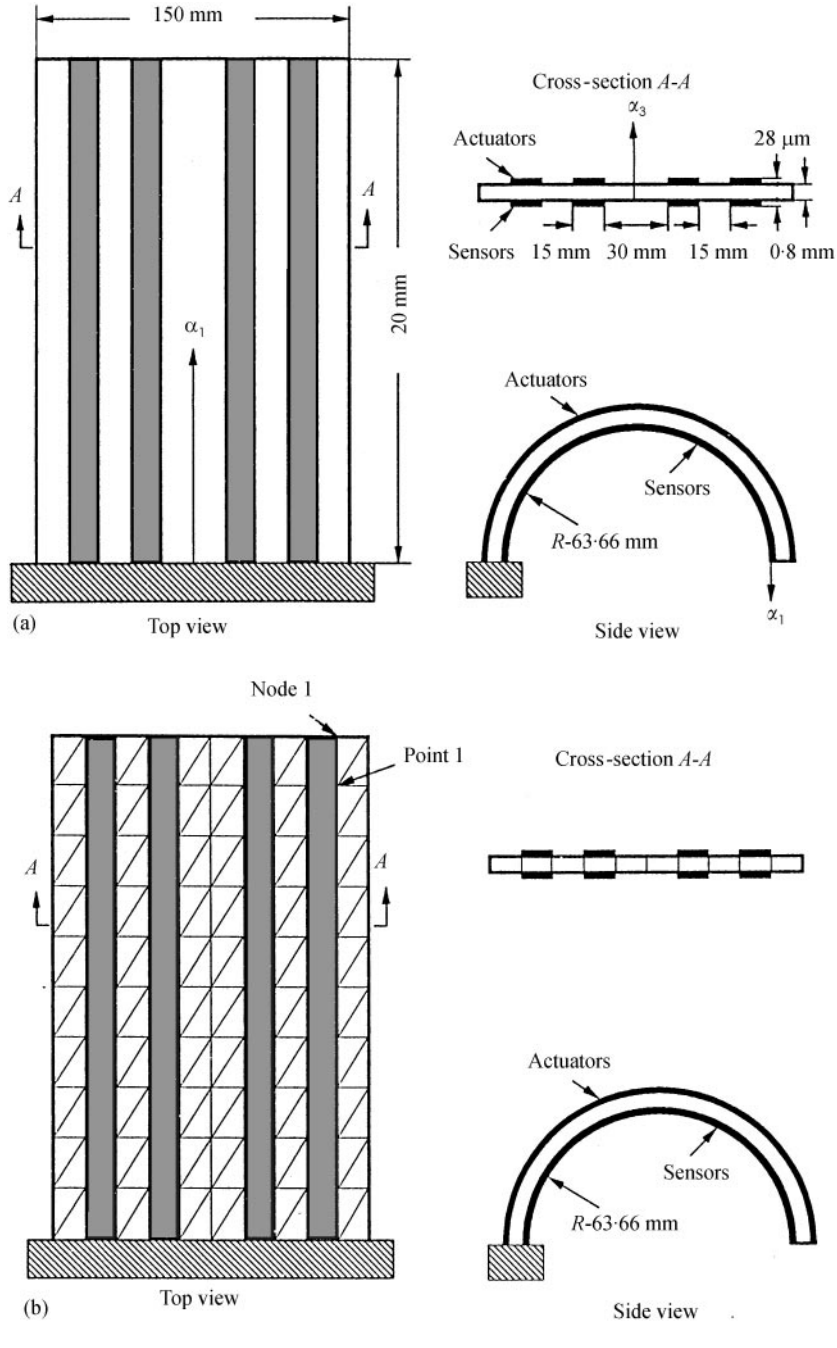

Figure 4. Piezoelectric laminated semicircular shell: (a) model and dimensions and (b) finite element modelling.

surface is $-10°C$ and the bottom surface is 10°C. Due to the thermal gradient shock of the two surfaces ($-10/10°C$), the shell oscillates and finally converges to a new equilibrium position. The negative velocity feedback control gains 0·0, $1{\cdot}0\omega_1$, $2{\cdot}0\omega_1$, and $5{\cdot}5\omega_1$ are used. Decay envelopes of free and controlled responses (the

TABLE 1

Material properties of steel and piezoelectric PVDF

Properties	Steel	PVDF	Units
Young's modulus, Y:	$0{\cdot}21 \times 10^{12}$	$0{\cdot}2 \times 10^{10}$	Pa
The Poisson ratio, μ:	0·3	0·29	
Density, ρ:	$7{\cdot}8 \times 10^{3}$	$1{\cdot}8 \times 10^{3}$	kg/m^3
Thermal conductivity, K:	35·0	0·17	W/m^{10} C
Thermal expansion, α:	$1{\cdot}1 \times 10^{-5}$	$1{\cdot}2 \times 10^{-4}$	$^\circ$C^{-1}
Piezo strain constant, d_{31}:		$2{\cdot}2 \times 10^{-11}$	m/V
Electric permittivity, ε_{11}:		$1{\cdot}062 \times 10^{-10}$	F/m
Pyroelectric constant, P_n:		$0{\cdot}25 \times 10^{-4}$	C/m^2/$^\circ$C
Capacitance, C:		$3{\cdot}8 \times 10^{-6}$	F/m^2

negative velocity feedback control with gains 0·0, $1{\cdot}0\omega_1$, $2{\cdot}0\omega_1$, and $5{\cdot}5\omega_1$) induced by the thermal shock are shown in Figure 7. All these responses should reach at the final steady state deflection, $(U_1, U_3) = (0{\cdot}16737$ cm, 0·135069 cm).

5.2.3. *Control of combined temperature and snap-back responses*

In this case, both the initial displacement (1 cm) and the thermal gradient shock ($-10/10^\circ$C) are considered as the input to the shell. Since the system is linear, the resulting responses are the summation of two individual responses and so the controlled responses. Free and controlled (gains 0·0, $1{\cdot}0\omega_1$, $2{\cdot}0\omega_1$, and $5{\cdot}5\omega_1$) displacement envelopes of node 1 are shown in Figure 8. Again, since there is a thermal gradient induced deflection, all responses converge to a final steady state equilibrium position $(U_1, U_3) = (0{\cdot}16737$ cm, 0·135069 cm).

6. CONCLUSIONS

Many mechanical and structural systems are working in a temperature-varied condition. Shell-type components and structures are very common parts in these systems. Modelling and control of these shell-type structures post many challenging issues. If piezoelectric materials are used as sensors and actuator, the study of piezothermoelastic materials and structures becomes necessary. In this paper, modelling, analysis and active vibration control of piezothermoelastic laminated shells are addressed and numerical examples demonstrated.

Piezothermoelastic constitutive equations, governing equations, and boundary conditions of a generic piezothermoelastic continuum were defined first. Finite element formulations of a new triangular piezothermoelastic shell element were presented and matrix equations of the piezothermoelastic shell laminated system were derived, in which mechanical, temperature, and electric couplings were defined. The electric force vector was used in active control of the shell laminates.

The newly developed triangular piezothermoelastic shell finite element was used to model a piezoelectric laminated composite plate to validate the new finite

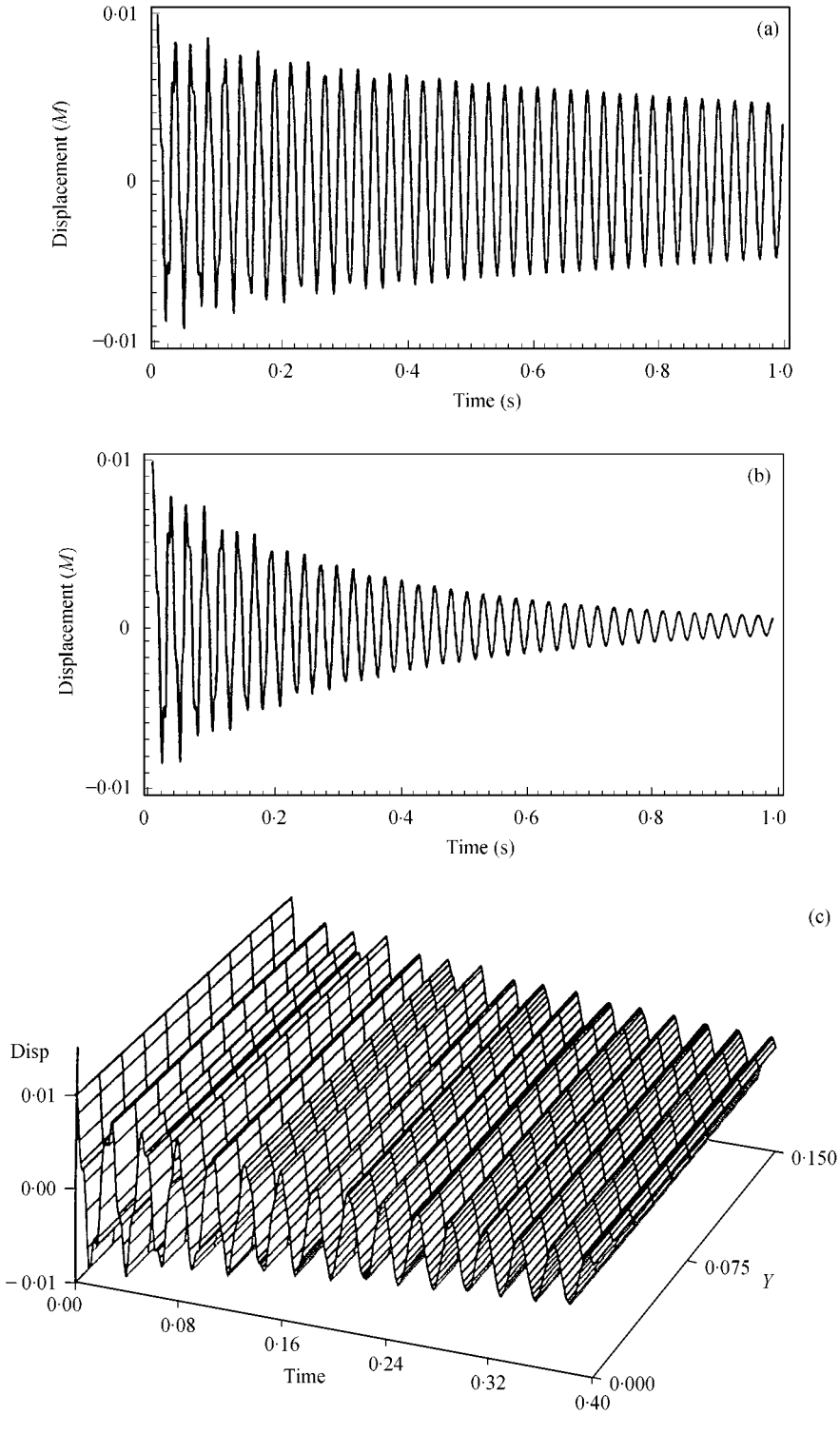

Figure 5. Free and controlled responses: (a) free snap-back response, (b) controlled response, and (c) 2-D controlled response of the free edge.

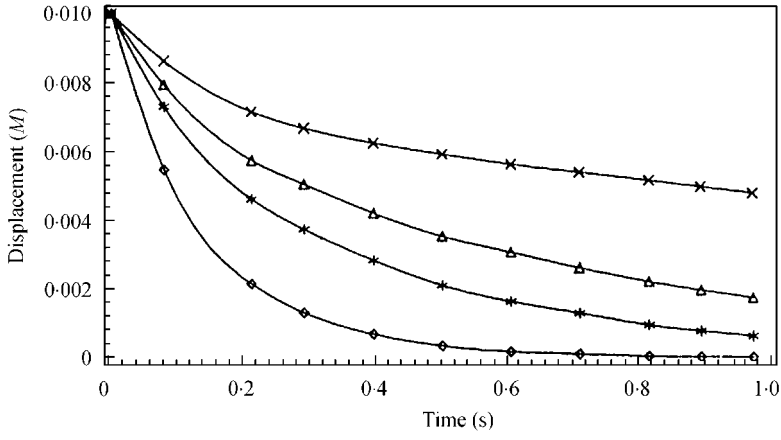

Figure 6. Comparison of free and controlled displacement envelopes (snap-back responses); ×, gain = 0·0; △, gain = 1·0; ★, gain = 2·0; and ◇, gain = 5·5.

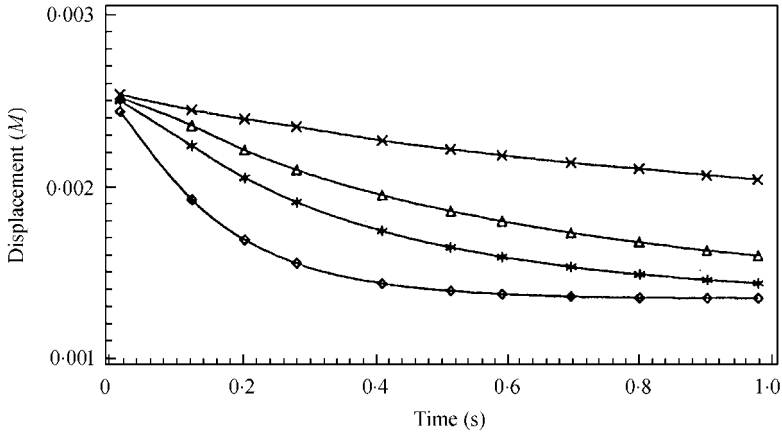

Figure 7. Comparison of free and controlled displacement envelopes (thermal shock responses): ×, gain = 0·0; △, gain = 1·0; ★, gain = 2·0; and ◇, gain = 5·5.

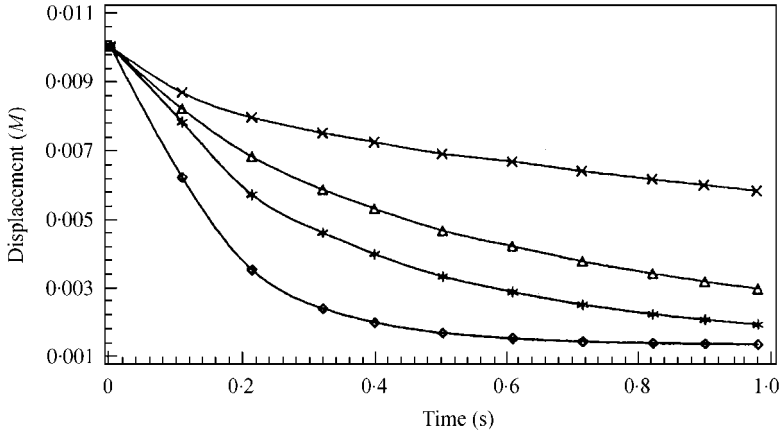

Figure 8. Comparison of free and controlled displacement envelopes (snap-back plus thermal shock responses): ×, gain = 0·0; △, gain = 1·0; ★, gain = 2·0; and ◇, gain = 5·5.

element code. Finite element solutions of the piezoelectric laminated composite plate were compared favorably with published experimental data and numerical solutions. Next the distributed control of a piezoelectric laminated semicircular shell subjected to mechanical and thermal shock excitations was investigated. Active control effects of the shell with mechanical and temperature excitations were studied. This study suggests that the newly developed finite element technique is capable for modelling and analyzing complicated piezothermoelastic shell systems. Distributed sensing and control effectiveness of piezoelectric laminated system can be studied and various design options evaluated.

ACKNOWLEDGMENT

This research was supported by a grant from the Army Research Office (DAAL-3-91-G0065, 1991–1994), technical monitor: Dr G. L. Anderson, and also a fellowship from the Center for Computational Sciences at the University of Kentucky.

REFERENCES

1. H. S. Tzou and G. L. Anderson 1992 *Intelligent Structural Systems*. Boston/Dordrecht: Kluwer Academic Publishers.
2. H. S. Tzou 1993 *Piezoelectric Shells* (*Distributed Sensing and Control of Continua*). Boston/Dordrecht: Kluwer Academic Publishers.
3. A. Baz and S. Poh 1988 *Journal of Sound and Vibration* **126**, 327–343. Performance of an active control system with piezoelectric actuators.
4. E. F. Crawley and K. B. Lazarus 1991 *AIAA Journal* **29**, 944–951. Induced strain actuation of isotropic and anisotropic plates.
5. J. E. Hubbard and S. E. Burke 1992 *Intelligent Structural Systems* (H. S. Tzou and G. L. Anderson, editors), 305–324. Boston/Dordrecht: Kluwer Academic Publishers. Distributed transducer design for intelligent structural components.
6. S. K. Ha, C. Keilers and F. K. Chang 1992 *AIAA Journal* **30**, 772–780. Finite element analysis of composite structures containing distributed piezoceramics sensors and actuators.
7. C. K. Lee 1992 *Intelligent Structural Systems* (H. S. Tzou and G. L. Anderson, editors), 75–167, Boston/Dordrecht: Kluwer Academic Publishers. Piezoelectric laminates: theory and experimentation for distributed sensors and actuators.
8. Y. Gu, R. L. Clark, C. R. Fuller and A. C. Zander 1994 *ASME Journal of Vibration and Acoustics* **116**, 303–308. Experiments on active control of plate vibration using piezoelectric actuators and polyvinylidene fluoride modal sensors.
9. H. S. Tzou, Z. P. Zhong and M. C. Natori 1993 *ASME Journal of Vibration and Acoustics* **115**, 40–46. Sensor mechanics of distributed shell convolving sensors applied to flexible rings.
10. H. S. Tzou, J. P. Zhong and J. J. Hollkamp 1994 *Journal of Sound and Vibration* **177**, 363–378. Spatially distributed orthogonal piezoelectric shell actuators (Theory and applications).
11. H. S. Tzou and R. V. Howard 1994 *ASME Journal of Vibration and Acoustics* **116**, 295–302. A piezothermoelastic shell theory applied to active structures.
12. D. Brei 1995 *Proceedings of the SPIE* 1995 *N.A. Conference on Smart Materials and Structures*, *San Diego*, *CA*. Force and deflection behavior for C-block piezoelectric actuator architectures.

13. H. S. Tzou and R. Ye 1994 *ASME Journal of Vibration and Acoustics* **114**, 489–495, Piezothermoelasticity and precision control of active piezoelectric laminates.
14. H. S. Tzou and R. Ye 1996 *AIAA Journal* **34**, 110–115. Analysis of piezoelastic structures with laminated piezoelectric triangle shell elements.
15. R. D. Mindlin 1961 *Problems on Continuum Mechanics* (J. Radok, editor), 282–290. Philadelphia: Soc. Ind. Appl. Math. On the equations of motion of piezoelectric crystals.
16. O. C. Zienkiewiez and R. L. Taylor 1989 *The Finite Element Method*, Vol. 1, fourth edition. New York: McGraw-Hill. Basic formulation and linear problems.
17. K. J. Bathe 1982 *Finite Element Procedures in Engineering Analysis*. Englewood Cliffs, NJ: Prentice-Hall.